7. MEASUREMENT OF INTENSITIES

less efficient than the scintillator, but, as in electron microscopy, the optical density is nearly proportional to the exposure. This explains the use of the Gd foil in neutron-diffraction topography.

If we take into account the possible inhomogeneity of the converter and the difficulties related to the film (homogeneity, development, and photodensitometry), an accuracy of 5 to 10% is achievable in the intensity measurements under good conditions.

Owing to the differences in the processes, neutron photographic techniques are much more efficient than those for X-rays. In the case of the plastic scintillator, the gain is about 10^3, which compensates for the much lower neutron fluxes.

7.3.4. Electronic aspects of neutron detection

7.3.4.1. *The electronic chain*

Each collected burst of electrons, corresponding to one captured neutron, will be successively amplified, identified (discriminated), and transformed to a well defined signal, by a chain of electronic devices that are represented in Fig. 7.3.4.1. In the case of the gas detector, the complete electronic chain is generally contained in a grounded metallic box acting as an electrical shield. The detector is connected to this box *via* a coaxial cable as short as possible to avoid noise and parasitic capacitance. A high-voltage power supply feeds the detector anode through a filter. The charge-sensitive preamplifier contains a field-effect transistor (FET) to minimize the background noise, since, from the detector up to this stage, the electronic level is very low. At the output of the FET, the pulse corresponding to one neutron has an amplitude of about 20 mV. This pulse enters an operational amplifier with adjustable gain G, which delivers a signal of about 2 V, the analogue signal (ANA). The electronic pulse-rise time (0.5 to a few µs) is adapted to the detector electron-collecting time, *i.e.* its amplitude is roughly proportional to the number of electrons collected at the anode. The last part of the electronic chain is a discriminator with an adjustable threshold, followed by a trigger delivering a calibrated signal (*e.g.* +5/0 V), called the logic signal (LOG), which is sent to a scaler.

In the case of the scintillator, the photomultiplier ensures the conversion of light to electrons and produces a strongly amplified electronic signal that is processed through a discriminator and trigger as for the gas detector.

7.3.4.2. *Controls and adjustments of the electronics*

For the gas detector, there are basically three parameters to be adjusted, the gas-amplification coefficient M (a function of the detector high voltage), the electronic amplification gain G, and the discriminator threshold T. Since these adjustments are interactive, the high voltage is initially set at the value given by the manufacturer. The gain G is adjusted in order not to saturate the amplifier. When the electronic amplifier power supply voltage is 5 V, a typical setting of the pulse maximum amplitudes is about 3 V.

We present now the three types of operation necessary to adjust the electronics.

(*a*) *Control of the pulse shape*. The analogue pulse ANA (see Fig. 7.3.4.1) is directly observed with an oscilloscope. Depending on the construction of the electronic chain, it is important to verify if the input of the oscilloscope (or of the multichannel analyser, see below) must be adapted with a 50 Ω impedance or not. This will ensure that the amplitude of the analogue pulse and the accessible value of the voltage threshold

are on the same scale (and not different by a factor of two). Fig. 7.3.4.2(*a*) shows characteristic shapes obtained when triggering the oscilloscope at, say, 0.2 V and observing a $^{10}BF_3$ gas detector either pulse by pulse or in a continuous way. This type of display allows the trained user to check the noise level, the amplitudes of the neutron pulses, the quality of the pulse shape, and the presence of any anomalous signal such as one due to flashes of parasitic electronic or electric noise (*e.g.* 50 Hz). γ rays produce fewer electrons than neutrons, so that the corresponding pulses are of a lower amplitude (by a factor of 1/5 to 1/20).

(*b*) *Control of the distribution of the pulse amplitudes*. The distribution of amplitudes of the various pulses in number of pulses per amplitude increment dN/dA is analysed and displayed using a multichannel analyser. Fig. 7.3.4.2(*b*) shows the amplitude spectrum for a $^{10}BF_3$ gas detector. The main peak at A_0 corresponds to the main neutron-capture reaction (2.3 MeV, 93%). From its FWHM, we define the detector electronic resolution $\Delta A/A_0$. The right-hand-side small peak is due to the 2.8 MeV, 7% capture reaction. The tail of amplitudes down to $4A_0/11$ corresponds to neutrons captured near the detector walls, which stop some of the secondary-particle trajectories (wall effect). The existence of a deep valley [see Fig. 7.3.4.2(*b*)] where the discriminator threshold T is placed ensures that all captured neutrons, and nothing else, are counted. The width of this valley guarantees good detection stability. Three effects might reduce this valley. Worsening of the gas quality will reduce all the pulse amplitudes (neutron and gamma), an increase in electronic noise will result in a resolution loss affecting the valley on both sides, and a high level of γ radiation will produce a pile up of the independent γ pulses, increasing their amplitude.

(*c*) *Optimization of the threshold and high-voltage values*. In order to set the threshold T at its optimum value for discrimination and stability, the total number of counts in the detector per unit time is plotted as a function of the threshold, for
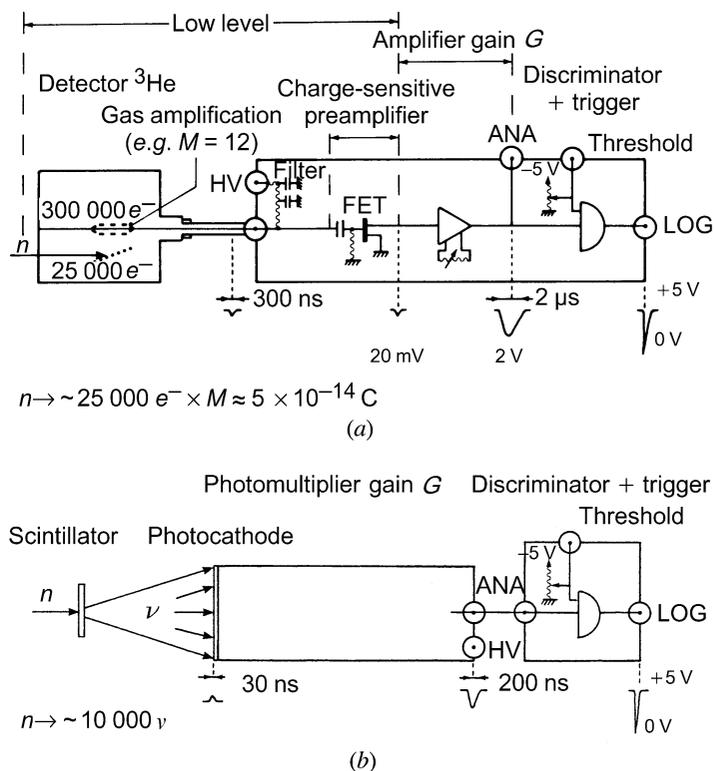

Fig. 7.3.4.1. Electronic chain following (*a*) an ^{3}He gas detector and (*b*) a scintillation detector.

648

a constant incident flux [see Fig. 7.3.4.2(c)]. On this curve, the width of the plateau and a value of the slope about 10^{-4} (in relative variation of counts per mV) give an indication of the detector quality. A good compromise is to set the threshold T at the middle of the plateau.

It is also necessary to verify that the detector high voltage, $i.e.$ the gas-amplification coefficient M (see Subsection 7.3.3.1), is well adapted. With the value of the threshold T adjusted as above, the number of counts per unit time is plotted as a function of the high voltage [see Fig. 7.3.4.2(d)]. Typical values for the width of the plateau and its slope are 200 V and a few per cent per 100 V. If the high-voltage setting given by the manufacturer must be modified (owing to the worsening of the gas or constraints from the electronic chain, $etc.$), the complete adjustment procedure of the G and T parameters must be repeated.

The electronic adjustments and controls of types of detector other than $^{10}BF_3$ gas detectors are basically the same once the changes in the amplitude spectrum have been taken into account. We present in Fig. 7.3.4.2(e) the amplitude spectra for an ^{3}He gas detector with significant wall effects, for a ^{10}B solid-deposit detector with very low efficiency, and for a scintillator. The energy of the secondary particles produced in an ^{3}He gas detector is 765 keV, about three times less than in $^{10}BF_3$, reducing the signal-to-noise ratio; the relative importance of the wall effect is greater and extends to $A_0/4$. In the case of the ^{10}B deposit detector, only one of the secondary particles escapes the foil, so that we do not detect an amplitude A_0 corresponding to the full capture-reaction energy, but only that corresponding

either to an average α or Li trace. The quality of the valleys depends on the t/r (foil thickness/particle range) ratio in the ^{10}B solid (see Fig. 7.3.3.2). The figure corresponds to a monitor where $t \ll r$. For the scintillator, the valley in the amplitude spectrum is not very good, even for good glasses and without γ radiation. The discrimination is therefore always much inferior to that of a gas detector. Moreover, the gain of the photomultiplier is very sensitive to the high voltage and has long-term stability problems.

7.3.5. Typical detection systems

7.3.5.1. *Single detectors*

In order to measure the scattered intensities, the single detector is mounted in a shield equipped with a collimator between sample and detector. The collimator is adapted to the sample (5 to 20′ Soller collimator for a powder diffractometer, or a hole adapted to the size of the beam diffracted by a single crystal). The sensitive area of the detector matches the size of the collimated diffracted beam. This geometry allows one to localize the scattered beam with adequate resolution and to avoid parasitic neutrons. In a powder diffraction measurement, the detector is scanned with a goniometer, each step being monitored.

7.3.5.2. *Position-sensitive detectors*

With the advantages of speed and simultaneity of data collection over broad angular ranges, position-sensitive detectors
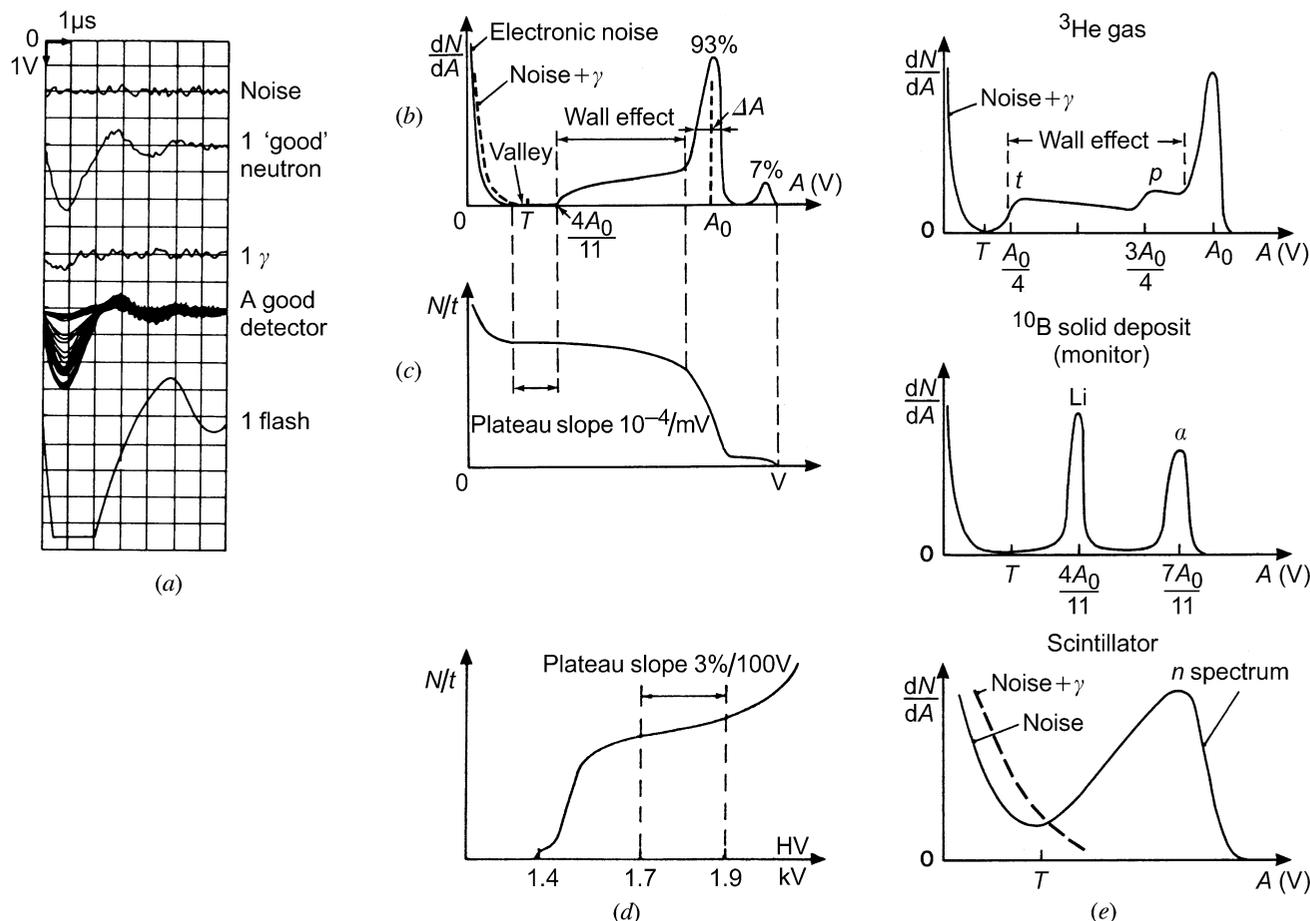

Fig. 7.3.4.2. (a) Characteristic $^{10}BF_3$ gas-detector analogue pulses seen on an oscilloscope. (b) $^{10}BF_3$ amplitude spectrum. (c) Plateau of a $^{10}BF_3$ detector as a function of the threshold voltage. (d) Typical plateau of a $^{10}BF_3$ detector in proportional mode as a function of the high voltage. (e) Amplitude spectra of various detectors.